Lattice dynamics and elastic properties of $LiPN_2$ and $NaPN_2$

2009 J. Phys.: Condens. Matter 21 405404

(http://iopscience.iop.org/0953-8984/21/40/405404)

J. Phys.: Condens. Matter **21** (2009) 405404 (7pp) doi:10.1088/0953-8984/21/40/405404

Lattice dynamics and elastic properties of $LiPN_2$ and $NaPN_2$

A V Kosobutsky

Physics Faculty, Kemerovo State University, Krasnaya 6, 650043 Kemerovo, Russia

E-mail: kosobutsky@kemsu.ru

Received 26 May 2009, in final form 10 August 2009
Published 8 September 2009
Online at stacks.iop.org/JPhysCM/21/405404

Abstract

Density functional theory calculations using the ultrasoft pseudopotentials and local density approximation have been carried out to investigate the phonon spectra and elastic properties of $LiPN_2$ and $NaPN_2$ crystals with chalcopyrite structure. As follows from the results obtained, phonon spectra of $LiPN_2$ and $NaPN_2$ consist of three bands and have a high-frequency boundary at $\sim$1200 cm^{-1}. Phonon modes of the upper half of the spectrum involve mainly nitrogen atom vibrations, whereas low-frequency modes have a predominant contribution from the lithium or sodium atoms and the contribution of phosphorus is almost uniformly distributed over the entire range of allowed frequencies. The calculations performed show that the dynamical and elastic behaviour of the compounds under study is determined by the strong covalent bond between P and N atoms and the substantially weaker interaction of the alkali metal and N atoms.

(Some figures in this article are in colour only in the electronic version)

1. Introduction

In the last few years many crystals from the large class of nitride compounds have gained considerable attention from researchers. As was shown in [1–4], such compounds as $LiPN_2$ and $NaPN_2$ are crystallized into the chalcopyrite structure (space group $I\bar{4}2d$) and characterized by unusually large tetragonal distortion in comparison with other chalcopyrite crystals. Owing to the possibilities of their practical use for producing diodes, solar elements, photodetectors and other devices of semiconductor optoelectronics, the crystals with a chalcopyrite lattice are of great interest and have been actively studied over several decades. Traditionally, the groups of chalcogenides $A^IB^{III}X_2^{VI}$ and pnictides $A^{II}B^{IV}X_2^V$ are included in this family. In contrast to the latter one, the formula of the compounds $A^IB^VX_2^V$ contains two different atoms from the fifth group of the periodic system; in the case of $LiPN_2$ and $NaPN_2$ they are phosphorus and nitrogen. This feature, as well as the presence of alkali metal atoms in the composition that determines high ionic conduction [5], makes them interesting for both experimental and theoretical studies.

Modern first-principles calculation techniques of electronic, elastic, dielectric and phonon crystal properties based on the density functional theory formalism have proven to be an effective research tool. The results of such investigations are highly reliable and have predictive power. For example, successful first-principles studies of the lattice dynamics properties of Cu- and Ag-based $A^IB^{III}X_2^{VI}$ crystals can be found in [6–9], while [10] presents phonon spectra and density-of-states calculations for three Li-containing $LiMTe_2$ (M = Al, Ga, In) compounds. It is worth noting that, on the whole, the lattice dynamics investigations of chalcopyrite crystals, both in coverage of the considered compounds and amount of obtained data, are still rather fragmentary. In many cases, due to the natural restrictions of such frequently used techniques as infrared and Raman spectroscopies and difficulties of the first-principles approach the experimental and theoretical studies are restricted to obtaining frequencies in the long wavelength limit. However, only thorough knowledge of phonon dispersion provides complete information about the dynamic properties of a compound and, from a theoretical point of view, gives the straightforward possibility of modelling of its thermodynamic properties.

The aim of the present work is to investigate the complete vibrational spectra and elastic properties of the chalcopyrite-type crystals from the $A^IB^VX_2^V$ group. Electronic band structure and zone-centre phonon modes of $LiPN_2$ and $NaPN_2$ have previously been studied theoretically in [11]. The present paper additionally provides the results of *ab initio* calculations of a full set of dynamic characteristics: Born effective charges, high-frequency dielectric constants, phonon dispersion relations, total and partial phonon densities of states

as well as elastic constants and bulk moduli of $LiPN_2$ and $NaPN_2$.

2. Computational details

Calculations of the phonon spectra of $LiPN_2$ and $NaPN_2$ compounds have been performed within density functional perturbation theory (DFPT) [12] using Vanderbilt ultrasoft pseudopotentials [13], a plane-wave basis and the local density approximation for the exchange–correlation potential. As is known, although the sodium atom has a simple electronic structure with only one 3s valence electron, there is a problem with its (and other heavy alkali metals) pseudopotential construction due to nonlinear exchange–correlation interaction between the core and valence charge densities which significantly overlap in Na. This problem can be partly solved by applying the nonlinear core correction [14]. In the present work we have preferred a direct and more accurate approach and a more complicated pseudopotential used for sodium, which in addition to the outer 3s electron explicitly treats as valence states also the eight electrons of 2s and 2p inner filled subshells of Na. This made it possible to trace more precisely the difference of $LiPN_2$ and $NaPN_2$ electronic properties and obtain lattice parameters of the latter closer to the experimental. All calculations in this work were carried out using the QUANTUM ESPRESSO code [15].

The electron wavefunctions were expanded in terms of a plane-wave basis set with a kinetic energy up to 35 Ryd, whereas the charge density cutoff was chosen 10 times as large. The Brillouin zone was sampled with a $4 \times 4 \times 4$ k-point mesh (with offset) generated according to the Monkhorst–Pack scheme [16] that corresponds to 11 special points in the irreducible wedge. The valence electrons of nitrogen are strongly localized and require a relatively high plane-wave cutoff to be treated properly when norm-conserving pseudopotentials are used. But ultrasoft pseudopotentials are computationally much less demanding; our test calculation in the centre of the Brillouin zone with energy cutoff increased up to 100 Ryd and on a denser mesh showed that the above-mentioned parameters are quite enough to yield the phonon frequencies converged to within 2 cm^{-1}. The most efficient way to obtain the phonon dispersion curves and density of states of complex compounds is to use a set of interatomic force constants that will be sufficient to give an accurate description of these properties. Modern methods rely on the Fourier-interpolation technique [12] which, by means of dynamical matrices calculation on a certain regular mesh in reciprocal space, allows us to produce force constants in real space and to use them in phonon mode evaluation at arbitrary k-points. The accuracy of the dispersion relations obtained in this way depends only on the density of the so-called q-mesh. In the present study for the force constants' generation a highly effective $4 \times 4 \times 4$ q-mesh (without offset) was employed.

3. Crystal structure

Calculations of vibrational modes have been carried out at optimized lattice parameters. As is well known, the chalcopyrite structure is characterized by three parameters: two lattice constants a and c and internal parameter u, which define the position of anions in the base plane of the unit cell (xy plane). It can be seen from table 1 that theoretical structural parameters agree quite well with experimental data. Here we have determined the u parameter for APN_2 compounds as $u = 1/4 + (d^2_{A-N} - d^2_{P-N})/a^2$, where d_{A-N} and d_{P-N} are the bond lengths between the corresponding atoms. In an ideal chalcopyrite lattice, which is a derivative of the sphalerite one, $u = 1/4$ and $c/a = 2$. For real compounds of chalcogenide $A^IB^{III}X^{VI}_2$ and pnictide $A^{II}B^{IV}X^V_2$ groups in most cases $u = 0.214$–0.304 and $c/a = 1.769$–2.016 [17]. Structural parameters of $LiPN_2$ and $NaPN_2$ have values going far beyond these boundaries. As is shown in table 1, the theoretical and experimental u values are within an interval 0.326–0.376, while the c/a ratio characterizing tetragonal distortion is within 1.403–1.625. Thus, the $LiPN_2$ and $NaPN_2$ crystals can be referred to as a distinct group of highly compressed chalcopyrite compounds.

Table 1. Theoretical and experimental structural parameters and interatomic distances.

	$LiPN_2$		$NaPN_2$	
Lattice parameters and bond lengths	Theory	Experiment [3]	Theory	Experiment [4]
a (Å)	4.462	4.575	4.915	4.972
c (Å)	7.250	7.118	6.948	6.976
c/a	1.625	1.556	1.414	1.403
u	0.3261	0.3301	0.3703	0.3761
d_{Li-N} or d_{Na-N} (Å)	2.045	2.093	2.361	2.409
d_{P-N} (Å)	1.634	1.645	1.634	1.639

There are significant differences between the structural parameters of $LiPN_2$ and $NaPN_2$. Obviously, the differences are related to various sizes of the alkali atoms. According to both theoretical and experimental data the replacement of Li atoms by the larger Na atom increases bond length between alkali metal and nitrogen atoms by 15%, whereas the P–N bond length changes very weakly—according to [4] a reduction by 0.4% occurs, while the theory predicts equal values $d_{P-N}(LiPN_2) = d_{P-N}(NaPN_2) = 1.634$ Å. A larger Na–N bond length results in increasing the u parameter in $NaPN_2$ by 14% as compared to $LiPN_2$.

4. Vibrational properties

The primitive unit cell of chalcopyrite crystal contains 8 atoms, therefore in the vibration spectrum there are 24 phonon branches. The D_{2d} group, which describes the chalcopyrite point symmetry, has four one-dimensional (A_1, A_2, B_1, B_2) and one two-dimensional (E) irreducible representations. A group-theoretical analysis gives the following decomposition of vibrational representation into its irreducible components at the Γ-point: $\Gamma_{tot} = A_1 + 2A_2 + 3B_1 + 4B_2 + 7E$. Acoustic modes are transformed as the irreducible B_2 and E representations; therefore for optical vibrations we have $\Gamma_{opt} = A_1 + 2A_2 + 3B_1 + 3B_2 + 6E$. Except for the A_2 silent mode, all the other modes are Raman-active. The infrared spectra are

Table 2. Born effective charges Z^* in atomic units.

Effective charges	$LiPN_2$	$NaPN_2$
Z^*_{Li} or Z^*_{Na}	$\begin{pmatrix} 1.02 & 0.05 & 0.00 \\ -0.05 & 1.02 & 0.00 \\ 0.00 & 0.00 & 1.03 \end{pmatrix}$	$\begin{pmatrix} 1.01 & 0.01 & 0.00 \\ -0.01 & 1.01 & 0.00 \\ 0.00 & 0.00 & 1.13 \end{pmatrix}$
Z^*_P	$\begin{pmatrix} 3.78 & -0.83 & 0.00 \\ 0.83 & 3.78 & 0.00 \\ 0.00 & 0.00 & 4.03 \end{pmatrix}$	$\begin{pmatrix} 4.15 & -0.92 & 0.00 \\ 0.92 & 4.15 & 0.00 \\ 0.00 & 0.00 & 3.80 \end{pmatrix}$
Z^*_{N1}	$\begin{pmatrix} -1.91 & 0.00 & 0.00 \\ 0.00 & -2.92 & -0.97 \\ 0.00 & -0.98 & -2.54 \end{pmatrix}$	$\begin{pmatrix} -1.88 & 0.00 & 0.00 \\ 0.00 & -3.30 & -1.13 \\ 0.00 & -1.15 & -2.48 \end{pmatrix}$
Z^*_{N2}	$\begin{pmatrix} -2.92 & 0.00 & -0.97 \\ 0.00 & -1.91 & 0.00 \\ -0.98 & 0.00 & -2.54 \end{pmatrix}$	$\begin{pmatrix} -3.30 & 0.00 & -1.13 \\ 0.00 & -1.88 & 0.00 \\ -1.15 & 0.00 & -2.48 \end{pmatrix}$

Table 3. High-frequency dielectric tensor components perpendicular to ($\varepsilon^{\perp}_{\infty}$) and along ($\varepsilon^{\parallel}_{\infty}$) the c axis.

ε_{∞}	$LiPN_2$	$NaPN_2$
$\varepsilon^{\perp}_{\infty}$	4.18	4.07
$\varepsilon^{\parallel}_{\infty}$	4.43	4.01

less informative because only B_2 and E modes belonging to the vector transforming representation can be experimentally observed. The A_1 and A_2 modes involve only nitrogen atom vibrations, whereas those of B_1, B_2 and E symmetry include displacements of the alkali and phosphorus atoms as well.

Phonon spectra of polar tetragonal crystals are characterized by splitting of infrared-active optical modes into longitudinal optic (LO) and transverse optic (TO) components with different frequencies, which results in discontinuities of the phonon branches in the Brillouin zone centre. The origin of these effects is the long-range macroscopic electric field accompanying atomic displacements [12]. The discontinuities occur for B_2 and E polar modes, while the frequencies of A_1, A_2 and B_1 modes do not depend on the direction of the Γ-point approach. The value of LO/TO splitting is determined by the Born effective charge tensors Z^* and high-frequency dielectric constant tensor ε_{∞} via a nonanalytic contribution to the force constants. The full set of these quantities is calculated within DFPT and no additional experimental data are required. Calculated components of Z^* and ε_{∞} are shown in tables 2 and 3, respectively.

The Born effective charge $Z^*_{k,\beta\alpha}$ measures the macroscopic polarization per unit cell created in direction β when all atoms of sublattice k are displaced in direction α, under the condition of zero electric field. As is known, the form of the effective charge tensor is determined by the atom site symmetry and, as can be seen from table 2, Z^* of all atoms have non-zero off-diagonal components. In the case of alkali atoms, Z^* off-diagonal components are very small, while the diagonal ones are practically equal to each other in $LiPN_2$ and have a difference of ~12% in $NaPN_2$. Note that the values of Z^*_{Li} and Z^*_{Na} diagonal components agree with the alkali metal atomic valence. From the comparison of the effective charge signs one can conclude that Li and P atoms play the role of cations, while N atoms act as anions. It should be noted that the dynamic charges for real systems do not coincide with the static atomic charges associated with the electron density transfer because of mixed ionic–covalent character of the material. However, due to the different electronegativity, the static displacement of the valence electron density in the directions from alkali atoms and P to N can be normally expected.

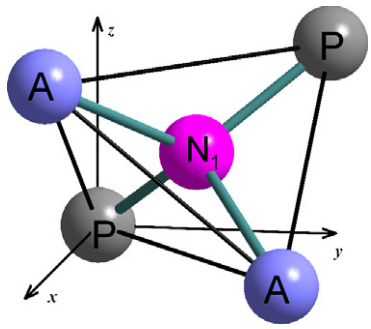

Figure 1. Distorted tetrahedral coordination of the nitrogen atom N_1 by two alkali (A) and two P atoms.

Effective charge tensors of P and N atoms have significant off-diagonal components, as well as display anisotropy of their diagonal terms. The largest diagonal term inequality is found for the nitrogen atoms. Thus, in the case of $NaPN_2$ depending on the displacement direction from the ideal position in the chalcopyrite structure specified by the u parameter, the values $Z^*_{N,xx} = -1.88$, $Z^*_{N,yy} = -3.30$ and vice versa are observed, while $Z^*_{N,zz} = -2.48$. Therefore, Z^*_N xx- and yy-component values are different by 1.42, indicating a significantly different electron polarization along the x and y axes when a nitrogen atom is displaced. There are no such substantial distinctions in the case of effective charges of 'traditional' chalcopyrites [6–10].

To find out the reasons for such strong Z^*_N anisotropy it is necessary to investigate the interactions of the nitrogen atoms with their environment. To be more specific, consider the N_1 atom (see table 2 and figure 1). Every nitrogen atom of the studied compounds is surrounded by two pairs of lithium (sodium) and phosphorus atoms located at the vertices of distorted tetrahedra. The nitrogen displacements along the three axes affect the interatomic bonds in different ways. Thus, in our coordinate system the N_1 atom displacement along the x axis in the positive direction leads to its equal distancing from the pair of phosphorus atoms and approaching the opposite

Table 4. Phonon frequencies in the Γ-point (cm^{-1}).

	$LiPN_2$	$NaPN_2$	
Symmetry	Theory	Theory	Experiment [18]
A_1	606	504	
A_2	1050	1102	
	514	445	
B_1	779	719	
	627	598	
	384	178	
B_2 (LO/TO)	1177/998	1165/1005	1150
	654/550	608/517	
	369/342	196/149	
E (LO/TO)	1176/1013	1204/1038	1050
	866/817	803/766	760
	600/553	611/554	570
	473/465	316/315	
	451/444	279/266	
	368/364	229/228	

pair of alkali atoms. The change of the electronic polarization induced by this shift determines the $Z^*_{N1,xx}$ value. The N_1 atom displacements along the y and z axes lead to its distancing from one pair of the Li (Na) and P atoms and approaching another such pair. These displacements determine the $Z^*_{N1,yy}$ and $Z^*_{N1,zz}$ components. Therefore, in comparison with $Z^*_{N1,yy}$ and $Z^*_{N1,zz}$ the significantly smaller absolute value of $Z^*_{N1,xx}$ indicates the weaker electronic structure deformation when the nitrogen is displaced from the nearest phosphorus atoms, in other words, it points to expressed covalent bond P–N and ionic bond Li–N (Na–N). This conclusion is confirmed by the electron density map calculations [11] which display common isodensity contours around and high density values between P and N atoms and small valence electron density at the alkali atom positions.

The mean values of the diagonal components of Z^*_P effective charge tensors are 3.86 for $LiPN_2$ and 4.03 for $NaPN_2$, while for Z^*_N charges they are −2.46 and −2.55, respectively. Hence, in comparison with the Li-containing compound, the Na-containing one is characterized by higher dynamic ionicity. As seen from table 3, in contrast to the effective charge tensor the electronic dielectric tensor is practically isotropic with the average values of its components 4.26 and 4.05 in $LiPN_2$ and $NaPN_2$, respectively.

Taking into account the LO/TO splitting of the polar B_2 and E modes, in table 4 the results of *ab initio* phonon calculations at the centre of the Brillouin zone are presented. Theoretical frequencies of $NaPN_2$ are compared with the observed ones, determined from the unpolarized IR spectrum measured in [18] between 400 and 4000 cm^{-1}. The data presented shows good agreement between the calculated and experimental zone-centre frequencies. Three most intensive absorption bands in the IR spectrum [18] at about 570, 760 and 1050 cm^{-1} can be assigned to the TO modes of E symmetry, while a weak shoulder near 1150 cm^{-1} corresponds to the LO mode B_2 symmetry. Taking into consideration the crystallochemical similarity of the compounds under study, we also expect good calculation accuracy for $LiPN_2$.

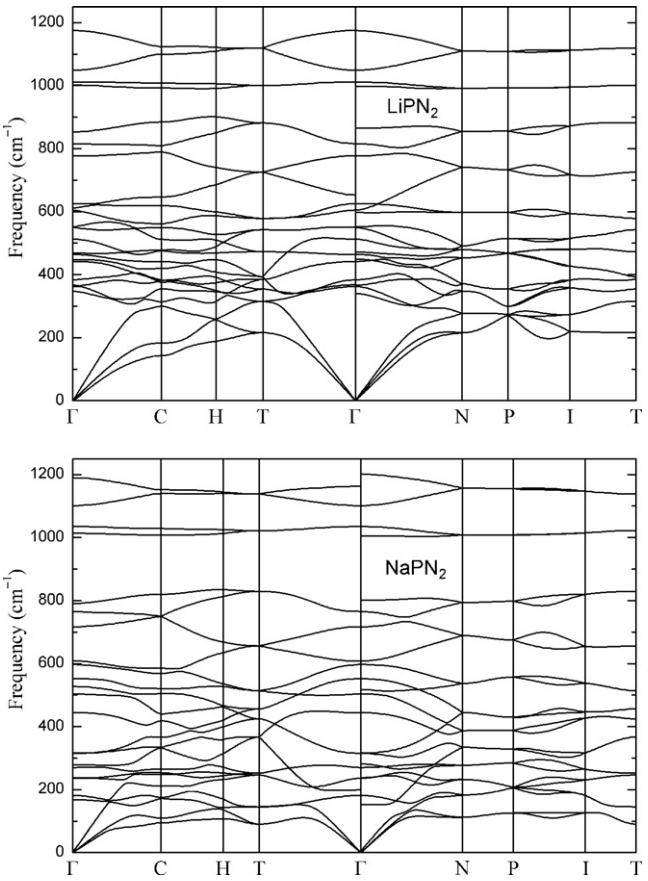

Figure 2. Phonon dispersion curves of $LiPN_2$ and $NaPN_2$.

The phonon dispersion curves calculated along several lines of the Brillouin zone and the corresponding densities of states are shown in figures 2 and 3. The phonon DOS is normalized to the number of phonons. Our calculations show that the spectra of both crystals consist of three bands and have the high limit at about 1200 cm^{-1}. The frequency boundary in $NaPN_2$ (1204 cm^{-1}) is located somewhat higher compared to $LiPN_2$ (1177 cm^{-1}). Thus, the frequency range of atomic vibrations in $LiPN_2$ and $NaPN_2$ is much wider than the typical 200–500 cm^{-1} for the $A^IB^{III}X^{VI}_2$ and $A^{II}B^{IV}X^V_2$ compounds [19]. As can be seen from figure 2, the vibrational branches have significant dispersion except for the two almost flat branches at ∼1000 cm^{-1} forming a separate narrow band which correspond to the strong double peak of ∼0.17 height in the density of states of both crystals. Higher halves of the spectra are in close proximity while lower ones exhibit considerable differences in the positions of the vibrational branches. On going from Li- to Na-containing compounds a sizeable downshift of the low-frequency branches by ∼200 cm^{-1} as well as softening of acoustic phonons along Γ–T, Γ–N and H–T directions take place. The differences in the branch positions appear in the density-of-states curves which have quite similar form only in the range above 650 cm^{-1}. The analysis of partial contributions to the density of states allows us to attribute the peculiarities observed to different participations of alkali, phosphorus and nitrogen atoms in the normal modes of low-and high-frequency

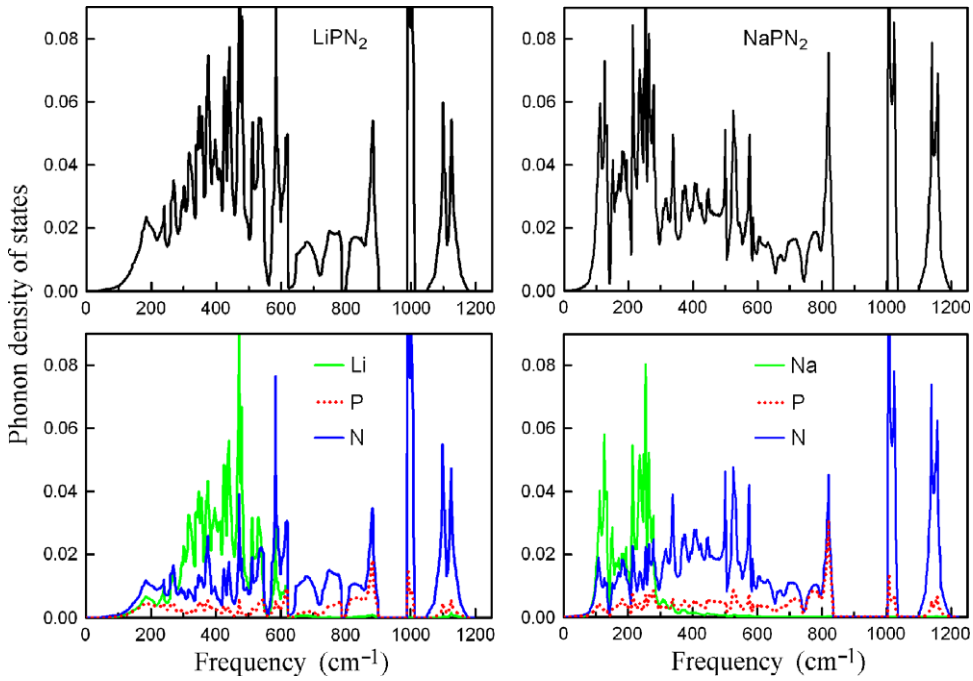

Figure 3. Total and partial phonon densities of states.

spectral ranges. Indeed, figure 3 shows that in the case of $LiPN_2$ within the range up to 560 cm^{-1} the Li atom vibrations make the primary contribution while in the higher modes those from the N atom predominate. The $NaPN_2$ density of states has twice as narrow an alkali atom vibration interval 0–280 cm^{-1} and a similar N atom contribution predominance in the rest of the spectrum. The contribution of the P atom, the heaviest of the three atoms of different types in the studied compounds, is almost equally spread all over the spectrum and can only be noticed within the intervals 800–900 cm^{-1} ($LiPN_2$) and 740–840 cm^{-1} ($NaPN_2$).

Taking into consideration the ratio of the Li, P and N atomic weights, such a distribution of the atomic displacements among the normal modes with various frequencies seems to be quite unusual. Indeed, as the lithium atom has the smallest weight of all three constituent elements, one could have expected that the range of the Li vibrations will be in the higher but not lower part of the spectrum. For example, the $LiMTe_2$ (M = Al, Ga, In) phonon spectra of Li-containing crystals with the chalcopyrite lattice demonstrate such a kind of phonon band structure [10]. The upper limit of the spectral range in these compounds does not exceed 372 cm^{-1}, which is much lower than the $LiPN_2$ and $NaPN_2$ frequency range limit and the bands of the Al, Ga, In and Te atom vibrations are lower than that of the Li atoms.

Evidently, the reason for the calculated frequency distribution of the atomic vibrations in $LiPN_2$ and $NaPN_2$ compounds is the large difference between bond forces of Li–N (Na–N) and P–N chemical bonds which also, as was demonstrated earlier, provides anisotropy of the Born effective charges. According to the obtained data we can make a general conclusion that the phosphorus presence in higher modes is the result of its considerably stronger bond with the nitrogen in comparison with the Li–N and Na–N interactions. Weak Li–N bond and the small size of the lithium atom explain the significant ionic conduction observed in $LiPN_2$ [5]. As the analysis of the effective charges has shown, the P–N interaction is of mainly covalent character. On the other hand, the strong LO/TO splitting of the B_2 and E higher polar modes indicates that the P–N bond also has a considerable ionic component.

5. Elastic properties

The elastic properties of the tetragonal crystals are characterized by six elastic stiffness constants c_{11}, c_{33}, c_{44}, c_{66}, c_{12} and c_{13}. To calculate these quantities we have used linear stress–strain relations. As a periodicity element, the crystallographic unit cell containing 16 atoms has been chosen and three types of strains were applied: the tetragonal, orthorhombic and shear. The cell deformation was specified by its stretching and compressing along a and c axes at 0.5–1%, as well as by shearing in xy and yz planes, characterized by angles of 0.5°–1°. The calculations of stress tensor components were made after optimization of atomic coordinates in a strained lattice. The numerical accuracy of the computation of stress tensors is known to depend sensitively on the choice of the plane-wave energy cutoff and the Brillouin zone sampling. We used the same plane-wave cutoff as for phonon frequency evaluation (35 Ryd) and a $4 \times 4 \times 2$ k-point mesh that allows us to obtain the elastic constants which are converged to better than 1 GPa, as a test calculation with doubled energy cutoff (70 Ryd) and a more dense k-point mesh have shown.

Based on the known c_{ij} values, it is easy to produce the linear compressibilities χ_a, χ_c along the a and c axes, volume

Table 5. Elastic constants c_{ij} (in GPa), linear and volume compressibilities χ_a, χ_c, χ (in TPa^{-1}) and bulk moduli B (in GPa).

	$LiPN_2$	$NaPN_2$
c_{11}	269.0	305.6
c_{33}	217.2	165.5
c_{44}	161.5	119.8
c_{66}	100.5	67.2
c_{12}	28.4	47.1
c_{13}	125.3	106.4
χ_a	2.77	1.65
χ_c	1.41	3.92
χ	6.95	7.22
B	144.0	138.4

compressibility χ and bulk moduli B [20]:

$$\chi_a = -\frac{1}{a}\frac{\partial a}{\partial p}\bigg|_{p=0} = \frac{c_{33}-c_{13}}{c_{33}(c_{11}+c_{12})-2c_{13}^2},$$
$$\chi_c = -\frac{1}{c}\frac{\partial c}{\partial p}\bigg|_{p=0} = \frac{c_{11}+c_{12}-2c_{13}}{c_{33}(c_{11}+c_{12})-2c_{13}^2},$$
$$\chi = -\frac{1}{V}\frac{\partial V}{\partial p}\bigg|_{p=0} = 2\chi_a+\chi_c, \qquad B = 1/\chi.$$

The evaluated elastic constants, as well as compressibilities and bulk moduli, are listed in table 5. To our knowledge, there are no other results, theoretical or experimental, available for comparison. The obtained c_{ij} values satisfy the Born stability criteria [21] for the tetragonal lattice: $c_{11}, c_{33}, c_{44}, c_{66} > 0$, $c_{11} > |c_{12}|$, $c_{11}c_{33} > c_{13}^2$ and $(c_{11}+c_{12})c_{33} > 2c_{13}^2$, thus implying that $LiPN_2$ and $NaPN_2$ crystals are mechanically stable.

As one can see from the data presented in table 5, both crystals have quite high elastic constants and bulk moduli in comparison with their structural analogues from $A^IB^{III}X_2^{VI}$ and $A^{II}B^{IV}X_2^V$ groups [22, 23]. Moreover, there are large differences between the constants c_{11} and c_{33}, c_{44} and c_{66}, c_{12} and c_{13}, respectively, whereas in many ternary compounds with chalcopyrite or related structures the pseudocubic elastic behaviour is observed [9, 22, 23]. Obviously, the strong anisotropy of the elastic constants exhibited by $LiPN_2$ and $NaPN_2$ is a consequence of the above-discussed difference in the interatomic bond strengths.

Almost all the elastic constants of $LiPN_2$ are substantially higher than the corresponding c_{ij} values of $NaPN_2$ with the exception of c_{11} and c_{12}, which grow at transition from Li- to Na-containing compounds. Therefore, the replacement of Li atoms by Na atoms strongly affects the elastic properties of $A^IB^VX_2^V$ crystals.

6. Conclusion

In this paper, the results of an *ab initio* study of the lattice dynamical and elastic properties of $LiPN_2$ and $NaPN_2$ compounds, being crystallized into the chalcopyrite structure have been reported. The calculations have been performed by using the state-of-the-art computational technique based on the density functional theory. The previous experimental investigations and our calculations show that $LiPN_2$ and $NaPN_2$ crystals have unusually large values of the tetragonal distortion $(2 - c/a)$, in the range of 0.4–0.6, and, therefore, form a separate group of highly compressed chalcopyrite-like compounds.

As follows from the computed phonon dispersion relations and densities of states, the phonon spectra of both crystals consist of three bands with a boundary at about 1200 cm^{-1}. Thus, the range of allowed frequencies in $LiPN_2$ and $NaPN_2$ is significantly wider than the typical 200–500 cm^{-1} for the isostructural $A^IB^{III}X_2^{VI}$ and $A^{II}B^{IV}X_2^V$ compounds. Low-frequency phonon modes have a predominant contribution of alkali atom vibrations, while in the upper part of the spectrum vibrations of the nitrogen atoms dominate and contribution of the phosphorus atoms is almost uniformly distributed over the whole spectrum. The participation of the light lithium atoms only in the low-frequency modes is due to their weak ionic bond with nitrogen against the background of the strong covalent bond between phosphorus and nitrogen in the PN_4 tetrahedra, forming a three-dimensional network structure of the studied compounds. Hence, our calculations serve as indirect confirmation of the high Li atom mobility in the $LiPN_2$ lattice and the possibility of significant ionic conduction of $LiPN_2$. The strong covalent bond between phosphorus and nitrogen manifests itself in the high position of the allowed frequency limit, Born effective charge anisotropy and large values of the elastic constants and bulk moduli.

Acknowledgments

This work was supported by the 'Development of Scientific Potential of the Higher School (2009–2010)' program of the Russian Ministry of Education and Science, registration no. 2.1.1/1230.

References

[1] Eckerlin P, Langereis C, Maak I and Rabenau A 1965 *Special Ceramics 1964* vol 3, ed P Popper (London: Academic) p 79
[2] Marchand R, L'Haridon P and Laurent Y 1982 *J. Solid State Chem.* **43** 126
[3] Schnick W and Lücke J 1990 *Z. Anorg. Allg. Chem.* **588** 19
[4] Landskron K, Schmid S and Schnick W 2001 *Z. Anorg. Allg. Chem.* **627** 2469
[5] Schnick W and Lücke J 1990 *Solid State Ion.* **38** 271
[6] Łażewski J, Parlinski K, Hennion B and Fouret R 1999 *J. Phys.: Condens. Matter* **11** 9665
[7] Łażewski J and Parlinski K 1999 *J. Phys.: Condens. Matter* **11** 9673
[8] Eryiğit R, Parlak C and Eryiğit R 2003 *Eur. Phys. J.* B **33** 251
[9] Gürel T and Eryiğit R 2006 *J. Phys.: Condens. Matter* **18** 1413
[10] Kosobutsky A V, Basalaev Yu M and Poplavnoi A S 2009 *Phys. Status Solidi* b **246** 364
[11] Basalaev Yu M, Kosobutsky A V and Poplavnoi A S 2009 *Semiconductors* **43** 735
[12] Baroni S, de Gironcoli S, Dal Corso A and Giannozzi P 2001 *Rev. Mod. Phys.* **73** 515
[13] Vanderbilt D 1990 *Phys. Rev.* B **41** 7892
[14] Louie S G, Froyen S and Cohen M L 1982 *Phys. Rev.* B **26** 1738
[15] Baroni S, Dal Corso A, de Gironcoli S and Giannozzi P http://www.quantum-espresso.org/

[16] Monkhorst H J and Pack J D 1976 *Phys. Rev.* B **13** 5188
[17] Jaffe J E and Zunger A 1984 *Phys. Rev.* B **29** 1882
[18] Landskron K 2001 Phosphor(V)-nitride durch Hochdruck-Hochtemperatur-Synthese *PhD Thesis* München, Ludwig-Maximilians-Universität, p 122
[19] Ohrendorf F W and Haeuseler H 1999 *Cryst. Res. Technol.* **34** 339
[20] Sirotin Yu I and Shaskolskaya M P 1982 *Fundamentals of Crystal Physics* (Moscow: Mir)
[21] Born M and Huang K 1954 *Dynamical Theory of Crystal Lattices* (Oxford: Clarendon)
[22] Neumann H 2004 *Cryst. Res. Technol.* **39** 939
[23] Łażewski J, Neumann H, Jochym P T and Parlinski K 2003 *J. Appl. Phys.* **93** 3789